Design and operational characteristics of a robotic Wilhelmy balance

ARTICLE *in* LANGMUIR · SEPTEMBER 1993

Impact Factor: 4.46 · DOI: 10.1021/la00033a033

5 AUTHORS, INCLUDING:

William Brittain
Texas State University
97 PUBLICATIONS **4,187** CITATIONS

Reprinted from LANGMUIR, 1993, 9.

Design and Operational Characteristics of a Robotic Wilhelmy Balance

Erwin A. Vogler,* Kendrick B. Spencer, and David B. Montgomery

Polymer Chemistry Department, Becton Dickinson Research Center, P.O. Box 12016, Research Triangle Park, North Carolina 27709

Lorraine M. Lander and William J. Brittain

Department of Polymer Science, University of Ohio at Akron, Akron, Ohio 44325

Received March 19, 1993. In Final Form: July 12, 1993®

A robotic Wilhelmy balance (plate method) that automates data acquistion from a multiplicity of liquid samples is described. The design employed a commercial XYZ translation stage to locate a force transducer over any one of an XY array of liquid-sample positions. Z motion performed the immersion/withdrawal cycles involved in measurement of contact-angle hysteresis curves. Data files corresponding to the individual hysteresis curves were analyzed batch-mode by computer according to algorithms specifically developed for this task. Utility of the robotic balance as an extension of available surface-science analytical tools was demonstrated in four general wetting applications: (i) measurement of liquid–vapor interfacial tensions ($\gamma_{(lv)}$) of water and organic fluids, (ii) determination of contact angles formed by these fluids on silane-treated glass and silicon–metal substrata, (iii) measurement of concentration-dependent $\gamma_{(lv)}$ for three surfactants and a protein (nonionic, Tween-80; anionic, Aerosol-OT; and cationic, cetyl dimethylethyl-ammonium bromide; human serum albumin, HSA), and (iv) monitoring Tween–80 and HSA adsorption kinetics to a silane-treated glass slide. These studies verified that a robotic balance approach could provide accurate contact angle and interfacial tension measurements of both organic liquids and aqueous surfactant solutions.

Introduction

The Wilhelmy balance is a widely applied technique for measuring liquid–vapor and liquid–liquid interfacial tensions.[1] Wilhelmy balance tensiometry is also very useful for the accurate determination of liquid contact angles on solid surfaces. In our laboratories, this technique is applied so routinely in characterization of model surfaces[2-4] and quantification of surfactant or protein adsorption to various materials[5,6] that we have sought means to automate data acquisition and analysis. Toward this end, computational procedures that allowed batch processing of Wilhelmy balance hysteresis curves were previously developed which greatly simplified data reduction.[7] Herein we describe a Wilhelmy balance robot that automates the data acquisition part of our instrumentation program. The overall objective was to explore feasibility of automated balance tensiometry as an extension of available surface-science tools rather than development of a finalized, high-precision instrument. In this paper we briefly describe the design and operation of a prototype robotic balance and discuss in detail results obtained with this unit in applications of general interest to those in the surface-science community involved in wetting measurements.

A typical Wilhelmy balance (plate method) consists of three main components as outlined in Figure 1A. A glass or metal plate, with or without a surface treatment of interest, is suspended by a torsion wire from a continuously-reading force transducer (a microbalance with milligram sensitivity). The motorized stage brings a single liquid sample into contact with the plate while a controller/recorder of some kind records force measurements (weight) and the stage position from a displacement transducer (LVDT). The controller might be as simple as an analog voltage supply to the motorized stage, and data can be captured on an ordinary servomotor XY chart recorder. Alternatively, more sophisticated computer control and data acquisition schemes can be used. In either event, plots of force *vs* depth for the immersion (advancing) and withdrawal (receding) modes are generated from the data. Advancing and receding interfacial tensions or contact angle measurements can be determined from these so-called *hysteresis curves* by graphical methods.[7-9] This approach becomes quite tedious when many different liquids are analyzed because of the number of separate manipulations involved. Subsequent data reduction is very time consuming without computerized analysis.

Figure 1B diagrams the Wilhelmy robot we have developed. There are two salient features that differentiate this design from the conventional one shown in Figure 1A. First, the transducer is mobile in the robotic approach, centered over any one of an array of sample positions by an XYZ translation stage. Second, there is no separate LVDT used to sense the relative position of the plate and fluid. This latter feature is important because it greatly simplifies device operation and calibration. Immersion depth is eliminated as a variable by algorithms specifically developed for this task.[7] The controller for the robot is a PC that sends instructions to stepper motors

* To whom correspondence should be addressed.

® Abstract published in *Advance ACS Abstracts,* September 1, 1993.

(1) Neumann, A. W.; Good, R. J. *Surf. Colloid Sci.* **1979**, *11*, 31.
(2) Vogler, E. A. In *Wettability*; Berg, J., Ed.; Marcel Dekker: New York 1993; pp 194–224.
(3) Lander, L. M.; Brittain, W. J., Foster, M. D.; Vogler, E. A. *Polym. Prepr. (Am. Chem. Soc., Div. Polym. Chem.)* **1992**, *33*, 1154.
(4) Lander, L. M.; Siewierski, L. M.; Brittain, W. J.; Vogler, E. A. *Polym. Prep. (Am. Chem. Soc., Div. Polym. Chem.)*, in press.
(5) Vogler, E. A. *Langmuir* **1992**, *8*, 2005.
(6) Vogler, E. A. *Langmuir* **1992**, *8*, 2013.
(7) Martin, D. A.; Vogler, E. A. *Langmuir* **1991**, *7*, 422.
(8) Smith, L. M.; Bowman, L.; Andrade, J. D. *Proceedings of the Durham, England Conference on Biomedical Polymers*, Durham, England, July 1982; Biological Engineering Society: London, 1982; p 279.
(9) Fryden, P.; Lee, J. H.; Park, J. M., Andrade, J. D. In *Polymer Surface Dynamics*; Andrade, J. D., Ed.; Plenum Press: New York, 1988; p 9.

0743-7463/93/2409-2470$04.00/0

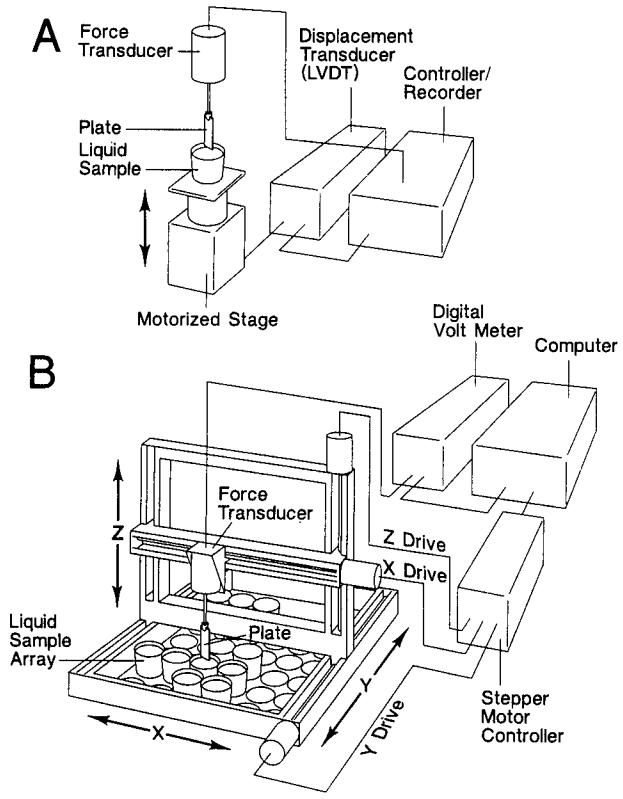

Figure 1. Diagrams of a conventional Wilhelmy balance (A) and the robotic Wilhelmy balance described herein (B). The robotic design differs from the conventional one in that the force transducer is centered over any one of an array of liquid-sample positions by and *XYZ* translation stage. No separate linear-voltage displacement transducer (LVDT) was used to directly sense the relative sample-liquid position. The *XYZ* translation stage was constructed from commercially-available stepper-motor-driven linear positioning components.

that drive the *XYZ* positioner. In operation, the transducer is positioned over a selected liquid-sample position (*XY* motion) and lowered or raised (*Z* motion) so that the plate is immersed into or withdrawn from the liquid, respectively. The robotic balance significantly simplifies analysis of many liquid samples by automatically scanning over each liquid sample location and recording transducer force measurements according to a preprogrammed set of instructions. Data corresponding to the individual hysteresis curves are stored and subsequently analyzed batch-mode as described previously.[7] See the Appendix for instrumentation details.

Methods and Materials

Substrata. Wettable glass plates (Clay Adams Gold Seal cover slips, 24 × 30 × 0.1 mm) used in Wilhelmy balance measurements of $\gamma_{(lv)}$ were prepared by sequential rinses in distilled water, 2-propanol, and Freon to remove putative surface contaminants followed by 15-min exposure to an oxygen plasma (100 W of 13.56-MHz RF power, ~50 mTorr of O_2). Silane-treated glass plates were prepared from cleaned cover slips by reaction with 2% octadecyltrichlorosilane (OTS, Hüills America) in $CHCl_3$ for about 1 h at ~60 °C in a sealed container. Silicon–metal substrata bearing close-packed hexadecyltrichlorosilane (HTS, Hüills America) self-assembled monolayers (SAMs) were prepared as described elsewhere.[3,4]

Solutions. Tween-80 (poly(oxyethylene) sorbitan monooleate, nominal MW = 1310, d = 1.064, used as received from Aldrich) and HSA (globulin-free lyophilized crystals, nominal MW = 69 000, used as received from Sigma Chemical) solutions were prepared in physiologic saline (Abbott, 0.9% USP). Cetyl dimethylethylammonium bromide (cetyl bromide, MW = 378.5, used as received from Aldrich) and sodium dioctyl sulfosuccinate (Aerosol OT or AOT, MW = 444.0, used as received from American Cyanamid) solutions were prepared in deionized and distilled water. No attempt was made to purify or check the purities of these test surfactants. In particular, HSA was not examined for the possible presence of surface-active contaminants such as poly(dimethylsiloxane) arising from the manufacturer's preparation procedures. However, we note that HSA interfacial properties were very similar to those of fetal bovine serum and freshly-prepared porcine plasma solutions that are overwhelmingly albumin in composition and free from purification artifacts.[2,5,6] The following organic fluids were used as received from Aldrich: 1-bromonaphthalene (98%), formamide (99%), diiodomethane (99%), octane (99+%), and tetrachloroethylene (99.9%). The following organic fluids were used as received from Fisher: trichlorofluoroethane (reagent), hexane, and pentane (Optima).

Results and Discussion

System Performance. As mentioned in the Introduction, our objective was to assess the feasibility of automated balance tensiometry as a surfactant-science tool rather than development of a high-precision instrument. Toward this goal we tested performance of the simply-constructed robotic balance diagrammed in Figure 1B and described in more detail in the Appendix. There are several engineering options that could be explored to improve performance of this prototype balance, particularly with respect to increasing the signal-to-noise ratio (S/N). Also, there are many different signal processing methods that could be applied to smooth data. However, none of these possibilities have been explored in this work. Instead, raw data collected at 20 data points/s with 1.5 mm/s *Z*-motion velocity at S/N ≈ 3000 are reported herein.

Figure 2 compares hysteresis curves so obtained using a fully wettable glass plate (advancing θ = receding θ = 0°, parts A and B) and a silicon metal wafer bearing an HTS self-assembled monolayer (SAM) (advancing θ = 112°, receding θ = 95°, parts C and D). The liquid phase was an aqueous saline solution (0.14 M NaCl). Parts A and C of Figure 2 plot force against sequential point number directly from the corresponding computer data file. Parts B and D of Figure 2 are the corresponding hysteresis curves in force–immersion depth coordinates retrospectively calculated sequential point number data according to methods described in ref 7. Immersion depth curves are shown in discrete point style with smoothed lines[10] drawn in to improve clarity of the repeat hysteresis curves. In either presentation style, the appearance of hysteresis curves is characteristic of either wettable or nonwettable surfaces. For nonwettable surfaces exhibiting contact angle hysteresis ($\theta_{adv} > \theta_{rec}$, Figure 2C,D), data corresponding to advancing (in) and receding (out) cycles are systematically offset on the force axis. By contrast, data recorded for highly-wettable surfaces exhibiting no contact angle hysteresis ($\theta_{adv} = \theta_{rec} = 0°$, Figure 2A,B) are not characteristically offset on the force axis. The principal utility of the data-point format is that the individual advancing/receding cycles, which are overlapping in immersion depth coordinates, are "unfolded" in point number space and can be individually analyzed.

Four different tests of the robotic balance are described herein. First, interfacial tensions of both water and organic fluids were repetitively measured and results compared to known values. Second, saline contact angle measurements on HTS SAMs measured by the robot were compared to those obtained using a commercial Wilhelmy balance (Cahn, Inc.) and to direct contact angle goniometer measurements. Contact angles of the organic fluids mentioned above on an OTS-treated glass plate were measured using the robotic balance, and a "Zisman plot"

(10) Procter, A.; Sherwood, P. M. *Anal. Chem.* **1980**, *52*, 2315.

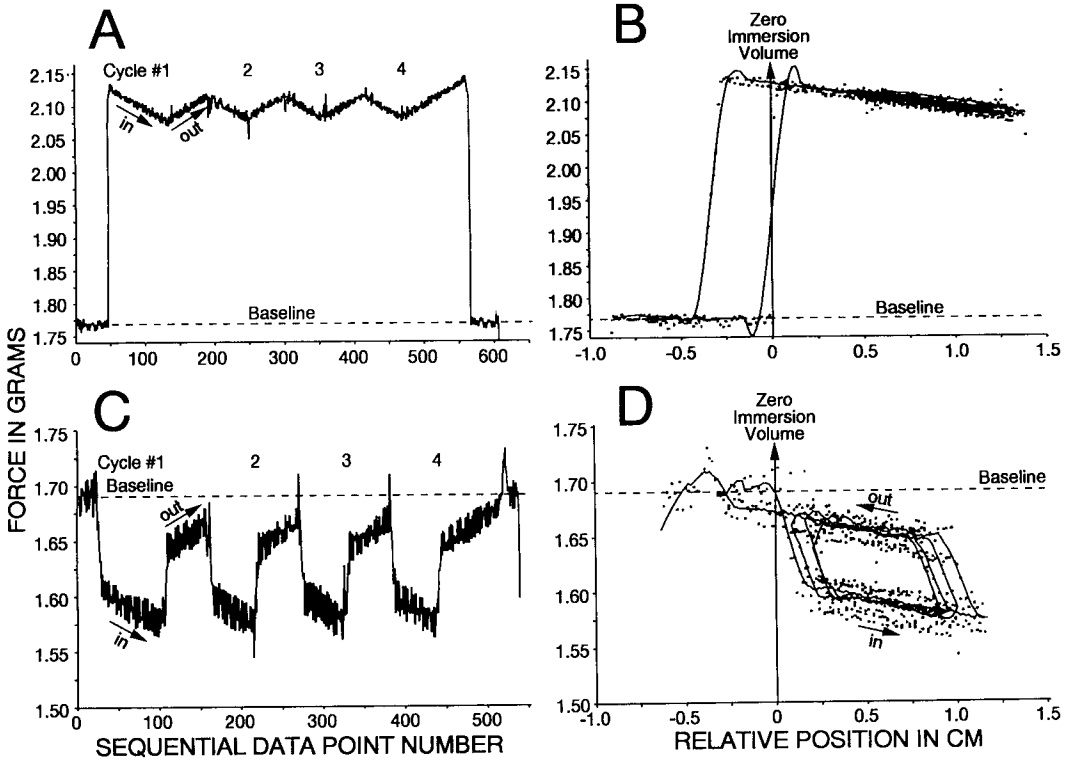

Figure 2. Hysteresis curves obtained with the robotic Wilhelmy balance for a perfectly wettable glass slide ($\theta_{adv} = \theta_{rec} = 0°$, parts A and B) and a nonwettable, silane-treated silicon–metal substrate ($\theta_{adv} > \theta_{rec}$, parts C and D) corresponding to advancing (in) and receding (out) cycles. Hysteresis curves in sequential point number space (A and C) were converted to conventional displacement coordinates (B and D) by algorithms specially designed for this task. Data spikes at direction reversals are due to the spring action of the vibration isolation mount described in the Appendix.

($\cos\theta$ against $\gamma_{(lv)}$) was constructed from the data. Third, concentration-dependent interfacial tensions were measured for nonionic, anionic, and cationic surfactants by both conventional and robotic methods. A single protein, human serum albumin (HSA), was selected for comparison to results obtained using the surfactant solutions. Resulting interfacial tension curves were quantitatively compared along with estimates of surface excess $\Gamma_{(lv)}$ obtained by applying Gibbs' adsorption isotherm to the data. Finally, application of the robotic balance in the study of adsorption kinetics is briefly described.

Interfacial Tensions of Aqueous Saline Solutions and Organic Fluids. The fundamental energetic measured in the Wilhelmy balance tensiometry is adhesion tension $\tau \equiv \gamma_{(lv)} \cos\theta$, where $\gamma_{(lv)}$ is liquid–vapor (lv) interfacial tension and θ is the contact angle. When $\theta \rightarrow 0$, the balance measures $\gamma_{(lv)}$ directly because $\cos\theta \rightarrow 1$ and $\tau \rightarrow \gamma_{(lv)}$. Table I compiles $\gamma_{(lv)}$ measurements for five sequential saline solutions, each analyzed using a four-immersion protocol (see Methods and Materials). A single, freshly cleaned and fully water-wettable glass plate was used for all five solutions. Parts A and B of Figure 2 correspond to results obtained with saline solution A in Table I. Columns 3 and 5 of Table I list the individual advancing and receding tension measurements. Columns 4 and 6 are the mean values for the four advancing/receding cycles on each of the five saline samples. Note that there was no statistically significant difference in results between cycles and among the five different saline solutions. The last row of columns 3 and 5 gives the mean tension values for all five saline solutions. From these mean values, it is apparent that advancing and receding cycles yielded identical measurements that were very close to the 72.8–73.0 dyn/cm anticipated for saline. This is taken as general confirmation of the accuracy of the robotic balance, at least for these aqueous saline solutions containing no surfactants.

Table I. Interfacial Tensions of Saline Solutions[a] by Robotic Wilhelmy Balance Tensiometry

		advancing $\gamma°_{(lv)}$ (dyn/cm)		receding $\gamma°_{(lv)}$ (dyn/cm)	
solution	cycle number	by cycle	mean ± std dev	by cycle	mean ± std dev
A	1	73.59 ± 1.05		73.77 ± 1.30	
	2	73.29 ± 1.26		74.44 ± 1.27	
	3	74.33 ± 1.32		74.28 ± 1.17	
	4	73.95 ± 1.19	72.79 ± 0.95	73.15 ± 1.03	73.91 ± 0.58
B	1	73.21 ± 1.61		73.67 ± 1.70	
	2	72.77 ± 1.71		73.10 ± 1.69	
	3	72.98 ± 1.77		73.15 ± 1.69	
	4	72.79 ± 1.73	72.94 ± 0.21	71.19 ± 1.60	72.78 ± 1.09
C	1	73.46 ± 1.13		72.96 ± 1.28	
	2	73.05 ± 1.26		73.49 ± 1.23	
	3	72.75 ± 1.34		72.49 ± 1.20	
	4	71.83 ± 1.28	72.77 ± 0.69	72.75 ± 1.12	72.92 ± 0.42
D	1	73.00 ± 2.87		73.23 ± 2.93	
	2	71.72 ± 3.02		73.51 ± 2.96	
	3	71.19 ± 2.99		71.63 ± 2.94	
	4	71.87 ± 3.00	71.94 ± 0.76	71.95 ± 2.86	72.58 ± 0.93
E	1	74.41 ± 0.99		74.19 ± 1.11	
	2	73.09 ± 1.31		71.48 ± 1.05	
	3	71.82 ± 1.28		69.52 ± 1.24	
	4	69.72 ± 1.03	72.26 ± 1.99	70.94 ± 0.96	71.53 ± 1.95
column means ± std dev		72.74 ± 1.12		72.74 ± 1.27	

[a] Abbott Laboratories, 0.9% physiologic saline.

Table II collects average advancing and receding $\gamma_{(lv)}$ measurements made on selected organic fluids and distilled water made with the robotic balance employing a single clean glass plate. Except for methylene iodide, there was no significant difference observed between advancing and receding modes, suggesting that $\theta \approx 0°$ in all but this case. Column 4 of Table II lists literature values[11] for these solutions for comparison to experimental results. Considering that no effort was made to purify these organic fluids, agreement is generally reasonable, again with the

(11) Shafrin, E. G.; Zisman, W. A. *J. Colloid Sci.* **1952**, 7, 166.

Table II. Interfacial Tension[a] of Organic Fluids[b] by Robotic Wilhelmy Balance Tensiometry

fluid	advancing $\gamma_{(lv)}$	receding $\gamma_{(lv)}$ (dyn/cm)	lit. value[c] (dyn/cm)
tetrachloroethylene	33.22 ± 2.27	33.04 ± 1.78	31.7
α-bromonaphthalene	35.70 ± 3.88	39.83 ± 3.80	44.6
methylene iodide	33.84 ± 2.08	40.70 ± 3.51	50.8
formamide	54.05 ± 3.08	54.18 ± 2.07	58.2
hexane	19.78 ± 1.24	18.68 ± 1.34	18.4
octane	18.66 ± 3.20	18.45 ± 2.72	21.8
pentane	18.21 ± 0.51	19.73 ± 0.04	16.0
water	72.93 ± 1.57	71.92 ± 0.89	72.8

[a] See Methods and Materials. [b] Average of two separate observations. [c] See ref 11.

Table III. Comparison of Conventional and Robotic Wilhelmy Balances in the Determination of Water Contact Angles on HTS Monolayers

	manual Wilhelmy balance[a]		robotic Wilhelmy balance[b]	
sample	θ advancing	θ receding	θ advancing	θ receding
A	111.8 ± 0.5	95.0 ± 0.3	111.3 ± 0.9	94.7 ± 1.1
B	112.3 ± 0.8	96.0 ± 0.4	106.7 ± 2.0	93.0 ± 3.2
C	113.1 ± 0.6	96.6 ± 0.4	110.9 ± 0.9	95.5 ± 1.3
column mean ± std dev	112.4 ± 0.7	95.9 ± 0.8	109.6 ± 2.6	94.4 ± 1.3

[a] Mean ± standard deviations of four individual hysteresis curves. [b] Mean ± standard deviation of four immersion cycles (see Results and Discussion and Figure 2).

exception of methylene iodide that exhibited the largest variance from accepted values. It is noteworthy in this connection that methylene iodide is subject to photolytic degradation, possibly producing surface-active impurities that were responsible for the difference between advancing and receding cycles (hysteresis) listed in Table II, and the variance from accepted values.

Measurements of Contact Angles. In the event $\gamma_{(lv)}$ is known, τ measurements can be converted to θ through $\cos^{-1}(\tau/\gamma_{(lv)})$. Table III compares results of advancing and receding contact angle measurements of saline ($\gamma_{(lv)}$ = 73 dyn/cm, see previous section) on three SAM surfaces. Results reported in Table III for sample A correspond to the data of Figure 2C,D. Using the conventional balance, it was not generally possible to analyze individual advancing/receding cycles that are overlaid in the force–immersion depth hysteresis curve presentation (as in Figure 2D). Consequently, results of four individual hysteresis curves were averaged for each SAM surface. By contrast, each cycle could be analyzed in point number coordinates (as in Figure 2C) using the robotic method. Corresponding results in Table III are mean values of four advancing/receding cycles. The two methods compare favorably, with the robotic balance yielding somewhat lower contact angles than the conventional method. Our experience with the conventional method is that graphical interpretation of hysteresis curves presented on a computer screen through the agency of vendor software is dependent on the positioning of graphics cursors and subjective user judgments of baseline position. Fully computerized analysis of hysteresis curves eliminates this subjectivity,[7] and we therefore conclude that robotic balance measurements are more reliable. In any event, differences between methods are negligibly small for most routine applications. Contact angles read directly by tilting-plate contact angle goniometry on eight similarly prepared substrata yield an average advancing θ = 110.3° ± 1.9° and receding θ = 90.3° ± 2.2°, in close agreement with the data of Table III.[4] These results confirm the accuracy of the robotic balance in the determination of contact angles from aqueous solutions containing no surfactants.

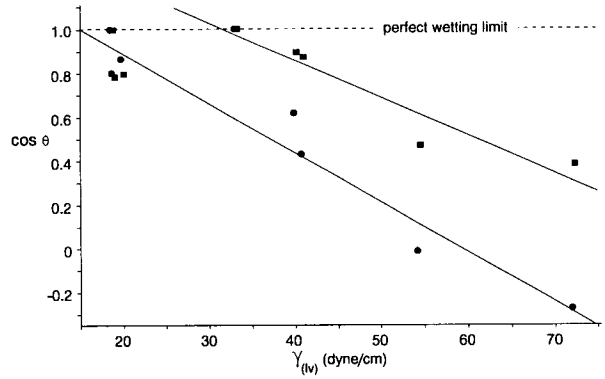

Figure 3. A Zisman plot constructed from contact angles of different organic fluids (see Table II) on a silane-treated glass slide (circles, advancing; squares, receding). Lines through the data represent best fits to the data measured up to the perfect wetting limit indicated by the dashed horizontal line. Note that overlapping cos θ_{adv} and cos θ_{rec} data points corresponding to perfect wetting have been slightly offset in the figure for clarity.

Contact angles of the organic fluids and water listed in Table II were measured on an OTS-treated glass plate using the robotic balance. It should be noted that these OTS-treated glass slides were not rigorously-prepared SAM surfaces. Results are shown in the Zisman plot of Figure 3 for both advancing and receding modes. Reasonably linear trends were obtained, and the advancing data were nearly parallel to the receding data. Trend lines shown in Figure 3 result from linear least-squares regression through advancing and receding data up to the point of perfect wetting, as noted by the horizontal line on the Zisman plot. Note that data corresponding to methylene iodide correlated reasonably well with those of the other fluids, suggesting that the $\gamma_{(lv)}$ value listed in Table II was accurate for this sample but different from literature values due to putative contaminants of unknown origin. However, advancing data corresponding to tetrachloroethylene (near $\gamma_{(lv)}$ = 33 dyn/cm) were completely wetting, spuriously out-of-line with all other data. This value was not used in the linear fitting of advancing contact angle data. The critical interfacial tensions γ_c for the advancing and receding modes calculated from the best-fit lines were 15.1 and 31.9 dyn/cm, respectively, as anticipated for a hydrophobic, silane-treated glass surface.

Concentration-Dependent Interfacial Tensions. These measurements are essential for the determination of Gibbs' surface excess, $\Gamma_{(lv)}$, which measures the amount of solute adsorbed at liquid–vapor interfaces.[2,5,6] We find this information very useful in understanding adsorption at interfaces, which is of critical importance in adhesion, biomedical, colloid, and surfactant sciences. Computational and experimental methods have been described in detail elsewhere.[5,6] Briefly recapitulating here for the present purposes, we measure $\gamma_{(lv)}$ of 24 serial dilutions of the surfactant of interest, starting with pure solvent and progressing through increasing concentrations to about 10% w/v. The robotic approach is ideal in this pursuit because it automates the repetitive $\gamma_{(lv)}$ measurements involved, and batch processing of the corresponding hysteresis curves by computer greatly simplifies data analysis. Ultimately, $\gamma_{(lv)}$ values so obtained are plotted against logarithmic dilution, and $\Gamma_{(lv)}$ values determined from the resulting *interfacial tension curve*. We further characterize these interfacial tension curves with four parameters denoted $\gamma^{\circ}_{(lv)}$, $\gamma'_{(lv)}$, $K_{(lv)}$, and $N_{(lv)}$.[6] The parameter $\gamma^{\circ}_{(lv)}$ measures $\gamma_{(lv)}$ at infinite solute dilution (solvent) whereas $\gamma'_{(lv)}$ measures the maximum surfactant effect (see annotations in Figure 4). The parameter $K_{(lv)}$

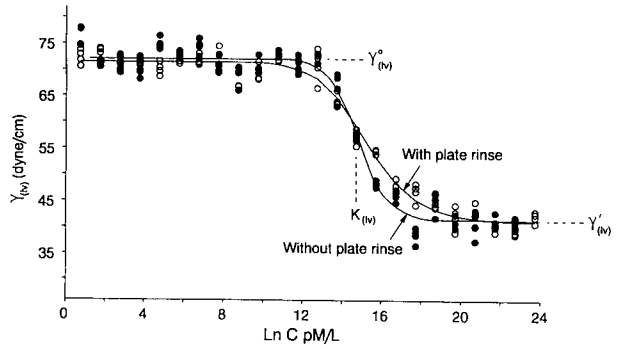

Figure 4. Interfacial tension curves for Tween-80 in saline measured by the Wilhelmy balance robot with (open circles) and without (closed circles) a plate-rinsing step between each solution in the dilution series (data correspond to solution 1 (A) listed in Table IV). Note that the nonrinsed data were systematically lower than those of the rinsed case within the Tween-80 concentration range $12 < \ln C < 18$ (C expressed as picomoles per liter, pM/L) where small changes in the Tween-80 concentration due to solution cross-contamination had a measurable effect. Annotations provide graphical interpretations of characteristic parameters listed in Tables IV and V.

measures the concentration at half-maximum change in $\gamma_{(lv)}$ whereas $N_{(lv)}$ is a measure of the steepness of the $\gamma_{(lv)}$ curve, with larger negative values for steeper slopes. These parameters can be tabulated, allowing quantitative comparison of interfacial tension curves.

Ideally, $\gamma_{(lv)}$ measurement by the plate method employs a rigorously clean and wettable plate for each solution to ensure the $\theta = 0°$ condition. The current robotic balance design does not permit automatic exchange of plates, so we tested the robotic approach both with and without an automatic plate-rinsing step between each $\gamma_{(lv)}$ measurement (rinse in pure water or saline as appropriate). The idea was to test the efficacy of a simple rinse compared with the ideal method. As before, robotic results were compared to those obtained using the conventional Wilhelmy balance, with a clean glass plate used for each individual surfactant solution in the dilution series.

Figure 4 compares interfacial tension curves for the same solutions of Tween-80 measured using the robotic Wilhelmy balance, with and without a plate-rinsing step. There were significant differences between rinsed and nonrinsed curves within the steeply-sloped portion of the $\gamma_{(lv)}$ curve. Table IV lists characteristic parameters for Tween-80 $\gamma_{(lv)}$ curves obtained with different batches of Tween-80 solutions identified in column 2. Differences between rinsed and nonrinsed interfacial tension curves are evident from the $K_{(lv)}$ and $N_{(lv)}$ parameters.

A proposal that can be advanced to account for the observed differences between rinsed and nonrinsed methods discussed above is that, in the nonrinsed case, small amounts of surfactant solution i carry over on the plate to the $i + 1$ solution, leading to a solution-to-solution contamination phenomena. Solution cross-contamination is consistent with the observation that differences between rinsed and nonrinsed cases were more pronounced at intermediate concentrations ($12 < \ln C < 17$ in Figure 4) where small changes in surfactant concentrations (particularly within the fluid meniscus microenvironment) can lead to large changes in $\gamma_{(lv)}$. Contamination of the $i + 1$ solution by the ith solution was apparently insignificant for solutions near the low- or high-concentration limits. Whatever the actual source of discrepancy is, nonrinsed methods consistently yielded steeper $\gamma_{(lv)}$ curves with higher uncertainties of fit (compare entries under $N_{(lv)}$ in Table IV). Larger slopes lead to exaggerated estimates of $\Gamma_{(lv)}$ from the nonrinsed interfacial tension curves (compare entries under $\Gamma_{(lv)}$ in Table IV).

Table IV. Interfacial Tensions for Tween-80/Saline by Method

		$\gamma^{\circ}_{(lv)}$ (dyn/cm)		$\gamma'_{(lv)}$ (dyn/cm)		$K_{(lv)}$ (ln C units)		$N_{(lv)}$		$\Gamma_{(lv)}$ (pmol/cm^2)	
method[a]	trial[b]	by trial	mean ± std dev	by trial	mean ± std dev	by trial	mean ± std dev	by trial	mean ± std dev	by trial	mean ± std dev
robotic balance	1 (A)	71.40 ± 0.40		42.02 ± 0.69		15.19 ± 0.16		−14.20 ± 1.38		243.87 ± 11.53	
with plate	2 (A)	70.80 ± 1.64		36.63 ± 1.41		15.65 ± 0.26		−10.84 ± 1.76		211.98 ± 16.82	
rinse	3 (A)	73.48 ± 0.69		38.30 ± 1.66		16.37 ± 0.27		−13.69 ± 1.55		261.91 ± 23.08	
	4 (B)	74.12 ± 0.74	72.45 ± 1.60	37.96 ± 1.34	38.73 ± 2.31	15.80 ± 0.27	15.75 ± 0.49	−10.64 ± 1.64	−12.34 ± 1.86	217.97 ± 16.20	233.93 ± 23.22
robotic balance	1 (A)	71.90 ± 0.49		42.82 ± 0.77		14.79 ± 0.14		−24.37 ± 3.81		423.55 ± 23.13	
without	2 (A)	71.32 ± 0.62		40.50 ± 1.13		15.26 ± 0.22		−17.73 ± 2.86		316.26 ± 22.60	
plate rinse	3 (A)	71.78 ± 0.52		37.68 ± 1.01		15.54 ± 0.19		−15.02 ± 1.68		292.68 ± 17.20	
	4 (B)	73.40 ± 0.74	72.10 ± 0.90	41.22 ± 1.08	40.55 ± 2.15	13.96 ± 0.24	14.89 ± 0.69	−12.97 ± 2.17	−17.52 ± 4.96	266.18 ± 18.87	324.67 ± 69.02
conventional	1 (C)	72.76 ± 0.24		40.05 ± 0.43		14.94 ± 0.09		−10.96 ± 0.62		213.21 ± 5.51	
balance with	2 (D)	72.66 ± 0.15		39.93 ± 0.24		14.83 ± 0.05		−12.91 ± 0.51		257.40 ± 3.85	
plate change	3 (E)	73.10 ± 0.21	72.84 ± 0.23	40.31 ± 0.33	39.92 ± 0.47	15.51 ± 0.07	15.06 ± 0.31	−13.96 ± 0.71	−12.51 ± 1.39	262.32 ± 5.49	244.31 ± 27.05

[a] See text for complete discussion of methods. [b] Letters in parentheses designate the solution set with different letters representing separate preparations.

Table V. AOT and HSA Interfacial Tensions by Method

surfactant system	method[a]	$\gamma^{\circ}_{(lv)}$ (dyn/cm)	$\gamma'_{(lv)}$ (dyn/cm)	$K_{(lv)}$ (ln C units)	$N_{(lv)}$	$\Gamma_{(lv)}$
AOT/H_2O	conventional balance	73.69 ± 0.38	23.36 ± 1.61	19.58 ± 0.16	12.66 ± 1.01	290.13 ± 16.66
	robotic balance	72.03 ± 0.58	20.61 ± 2.14	19.66 ± 0.22	13.18 ± 1.62	306.61 ± 22.95
HSA/saline	conventional balance	73.18 ± 0.40	52.93 ± 4.91	19.72 ± 1.28	10.42 ± 2.01	124.06 ± 17.16
	robotic balance	74.04 ± 0.64	60.84 ± 1.48	14.61 ± 0.54	11.58 ± 6.31	93.01 ± 19.70

[a] See text for complete discussion of the methods.

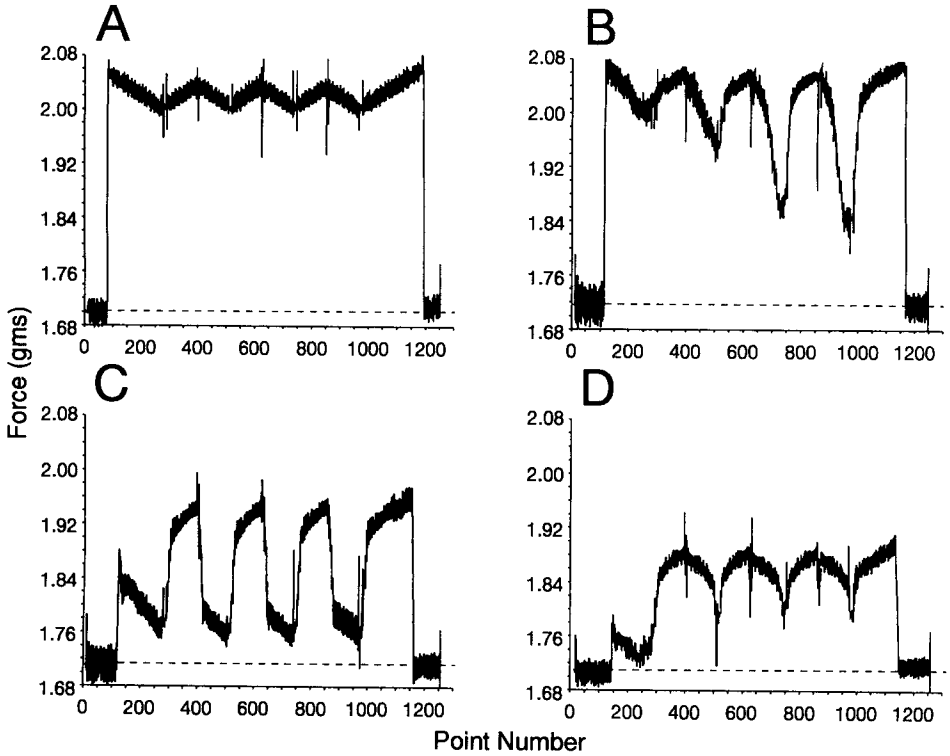

Figure 5. Evolution of contact angle hysteresis on a wettable glass plate dipped in increasing concentrations of cetyl bromide due to adsorption of this surfactant. For the most dilute solution (A), no contact angle hysteresis was observed, as evident from the regularity of the hysteresis curve (compare with Figure 2A). At higher concentrations (B), hysteresis was observed and was not stable, progressively changing with each advancing cycle and never attaining a repeatable advancing buoyancy slope. Hysteresis was much weaker at intermediate concentrations (C). At the most concentrated solution examined (D) hysteresis nearly disappeared.

Table IV also compares results of the robotic method to results obtained using conventional Wilhelmy balance tensiometry in which a freshly-cleaned glass plate was used for each solution in the Tween-80 dilution series. Conventional balance results correspond closely on an average basis to those obtained using the robotic balance with plate rinsing, with respect to both the characteristic parameters $\gamma^{\circ}_{(lv)}$ $\gamma'_{(lv)}$, $K_{(lv)}$, and $N_{(lv)}$ and the calculated value for $\Gamma_{(lv)}$. However, the robotic balance results were less precise by about a factor of 5, which is undoubtedly due to noise introduced by moving the sensor head in the robotic approach (see Appendix). Similar agreement between the robotic and conventional balances was obtained for the anionic detergent AOT and the protein HSA, as summarized in Table V.

It is concluded from the data of Tables IV and V that the plate-rinsing step was effective in eliminating solution cross-contamination and that neither surfactant nor protein was irreversibly adsorbed to the plate so that $\theta \approx 0$ for all solutions in the dilution series. This conclusion is entirely consistent with mechanistic studies of adsorption that suggest that neither surfactant type (nonionic and anionic) nor albuminoid proteins adsorb to water-wettable surfaces.[5,6]

Results for the cationic surfactant cetyl bromide were not so straightforward, however. In this case, the simple plate-rinsing step was ineffective and significant contact angle hysteresis was noted for all but the most dilute or concentrated cetyl bromide solutions, suggesting that $\theta > 0$ due to adsorption effects. Parts A–D of Figure 5 show the evolution of contact angle hysteresis in progression from dilute to concentrated solutions. For the most dilute solution (Figure 5A, 2.7×10^{-10}%), no contact angle hysteresis was observed, as evident from the regularity of the hysteresis curve (compare with Figure 2A), leading to an average $\gamma_{(lv)} = 73.62 \pm 0.97$ for four receding cycles, in agreement with values anticipated for an essentially surfactant-free solvent (water). At higher concentrations but still quite dilute (Figure 5B, 5.6×10^{-6}%), hysteresis was observed and was not stable, progressively changing with each advancing cycle and never attaining a repeatable advancing buoyancy slope. Hysteresis was much weaker at intermediate concentrations (Figure 5C, 2.4×10^{-3}%). At the most concentrated solution examined (Figure 5D, 2.6%) hysteresis nearly disappeared, but $\theta = 0°$ could not be assured for accurate $\gamma_{(lv)}$ determinations. These observations are entirely consistent with mechanistic studies of cetyl bromide adsorption[5] which suggest that the cationic head group of this surfactant strongly interacts with putative anionic functionalities on clean glass, leading to a head-down adsorption configuration that extends nonwettable moieties into solution. As a result, an *increasing contact angle* was observed with *increasing cetyl bromide concentrations.*

It is generally concluded from the study of nonionic, anionic, and cationic surfactants as well as albumin that the robotic balance can be used for reliable concentration-dependent $\gamma_{(lv)}$ measurements using a simple plate-rinsing

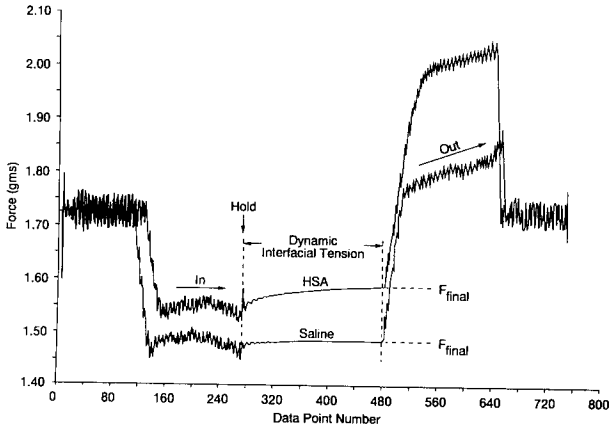

Figure 6. Force curve for the "dip-and-hold" method of measuring time-dependent interfacial tensions for saline (lower curve) and HSA solutions (upper curve). Data within the range denoted dynamic interfacial tension show a change in force due to hydrodynamic effects and adsorption to the silane-treated glass plate used in the study. This data range is shown in normalized force coordinates in Figure 7, calculated using extrapolated force values labeled F_{final} for saline and HSA (see text for discussion of computational procedures).

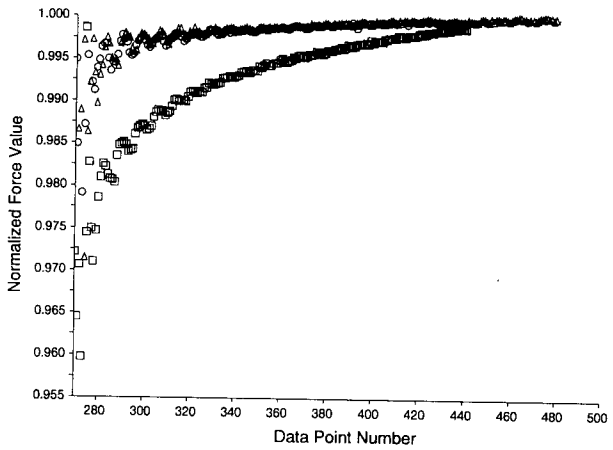

Figure 7. Adsorption dynamics for saline (circles), Tween-80 (triangles), and HSA (squares) expressed in normalized force units, illustrating relatively slow HSA adsorption kinetics of a silane-treated glass slide. HSA and saline data were extracted from the range labeled dynamic interfacial tension in Figure 6 (see text for discussion of computational procedures).

protocol, so long as there is no strong adsorption of surfactant to the plate. Adsorption can be detected by examining hysteresis curves as a function of surfactant or protein concentration. In those events where $\theta = 0°$ cannot be assured, a clean glass plate must be employed for each solution in the surfactant dilution series. Alternatively, the DuNouy ring method can be applied which is much less sensitive to nonzero contact angle effects.[1]

Dynamic Interfacial Tensions. Adsorptions kinetics is frequently of interest to those studying surfactants and proteins because information regarding the size, flexibility, and stability of solutes at interfaces can be deduced (see ref 12 and citations therein). As an example application of the robotic Wilhelmy balance in this pursuit, we examined time-dependent interfacial tensions due to adsorption of Tween and HSA to hydrophobic, silane-treated glass slides (surfactant concentrations at 2.6% w/v). The strategy was to simply immerse a silane-treated glass slide into the solution of interest to an arbitrary depth (approximately 1 cm) and monitor wetting forces as a function of time. Saline solutions served as controls in both the Tween-80 and HSA cases.

Figure 6 is a sequential point number curve obtained with the above "dip-and-hold" protocol for saline (lower curve) and HSA (upper curve), using OTS-treated glass slides. Data corresponding to that portion of the curve labeled "dynamic interfacial tension" (from data point number n = 270 to n = 480) were transformed into normalized force values by reference to the final force reading (force at n = 480, F_{final} in Figure 6) so that data for different test liquids could be compared on the same scale. A more rigorous data treatment would probably be required for a formal kinetic analysis, but for the purpose of illustrating application of the robotic balance, this simple normalization is adequate. Figure 7 compares results so obtained for saline, Tween, and HSA solutions. Tween and saline behaved nearly identically, with force values asymptotically reaching final values quite rapidly. By contrast, the rate of force change was considerably slower in the HSA case.

For saline with no added surfactant, adsorption kinetics can be ruled out as a cause of the observed time-dependent changes in force. It is reasonable to conclude that these dynamics were due to relaxation of the maximal advancing angle obtained during plate immersion to a lower, metastable value after motion of the plate through the liquid was discontinued, as well as to related changes in plate buoyancy. Saline thus can serve as a control for adsorption studies of Tween and HSA, representing the "background" hydrodynamic effects.

Separate studies of the interaction of Tween-80 solutions with hydrophobic surfaces confirms adsorption to silane-treated glass plates.[2,5,6] With this in mind, it is interesting that the interfacial dynamics observed for Tween-80 were nearly identical to those of saline. It must be concluded, therefore, that transport of Tween molecules to the microenvironment of the meniscus and subsequent adsorption to the saline-treated plate occur much more rapidly than the time frame of the kinetic measurements and were thus transparent to the observer. Adsorption of HSA to hydrophobic surfaces has also been confirmed in these previous studies. This fact, taken together with the slow rate observed in the HSA interfacial dynamics, leads to the conclusion that mass transport and adsorption of HSA were significantly slower than the time frame of the balance kinetic experiments, in sharp contrast to the results observed for Tween-80. Detailed kinetic analysis would be required to definitively differentiate between rate-limiting mass transport and rate-limiting adsorption steps for HSA.

It is concluded from this limited study of interfacial adsorption dynamics that the robotic Wilhelmy balance has general applicability to the study of adsorption kinetics.

Conclusion

Design and operation of a robotic Wilhelmy balance that automates data acquisition have been tested in four general wetting applications: (i) measurement of liquid–vapor interfacial tensions $\gamma_{(lv)}$ of water and organic fluids, (ii) determination of contact angles formed by these fluids on silane-treated glass and silicon–metal substrata, (iii) measurement of concentration-dependent $\gamma_{(lv)}$ for three surfactants and an albuminoid protein, and (iv) monitoring of adsorption kinetics. These studies demonstrated the general utility of a robotic balance as a surface-science tool. The particular balance design tested herein utilized a moving force transducer that was located over one of an array of liquid samples according to a preprogrammed set of instructions sent to a computer-controlled XYZ trans-

(12) Vogler, E. A. *J. Colloid Interface Sci.* **1989**, *133*, 228.

lation stage. The significant limitation of this design was transmission of vibrations to the force transducer during measurements that degraded the signal-to-noise ratio and introduced imprecision in the final measurements. Having verified the utility of a robotic Wilhelmy balance concept, however, it is concluded that exploration of more sophisticated instrument designs is warranted.

Acknowledgment. The authors are indebted to Ms. J. C. Graper for her skilled technical assistance.

Appendix

Instrumental Details. The *XYZ* translation stage was constructed from commercially available stepper-motor driven, screw-drive positioning equipment ("Unislide", VELMEX Inc., Bloomfield, NY; 51-cm travel lengths) which was supported on a vibration-isolation table (Newport Inc., Mountain Valley, CA). A Velmex 800 series stepping-motor controller was used to control the *XYZ* stage. The stepper-motor controller was programmed using a 486/33-MHz PC through the agency of Assyst software (Assyst Software Technologies Inc., Rochester, NY). The force transducer was a Scientech 202 electronic balance (Scientech Inc., Boulder, CO). Electronic balance preamplifier output was read by an HP 3457A digital multimeter (Hewlett-Packard, Palo Alto, CA) connected to the PC through an IEEE-488 port. Data read at programmable rates (0–20 data per second) were stored and processed on a VAX 9000 computer system (Digital Equipment Corp., Maynard, MA) directly linked to the PC through a local area network. Data processing was accomplished through programs written in RPL, a facility of the RS/1 information-handling software (Bolt, Barnak, and Newmann, Inc., Cambridge, MA) residing on the VAX computer. A system diagram is shown in Figure 1B.

The significant drawback of this instrument design was movement of the force transducer on a stepper-motor screw-drive vehicle. Vibrations transmitted to the sensor was sufficiently severe that a vibration-isolation mount for the transducer was required. This mount was constructed from two massive lead bricks separated by rubber pads and springs. The sensor was attached to the upper brick and was thus mechanically decoupled from the *XYZ* state, conferring a degree of vibration isolation from the screw-drive mechanism. It was noted that the signal-to-noise ratio (S/N, here taken to be the ratio of the mean voltage output to the standard deviation of the voltage signal) varied as a function of immersion velocities. In particular, S/N at *Z*-motion velocity near 0.2, 0.8, and 2 mm/s was significantly poorer than at other speeds. Apparently, the transducer mount was not effective in filtering vibrations that occurred at these velocities. Nevertheless, S/N > 3400 could be obtained within a useful range of *Z*-motion velocities between 1 and 2 mm/s, which is adequate for the purpose of testing the robotic Wilhelmy balance concept. Higher and lower velocities could be employed at S/N > 1000. Another drawback related to moving the force transducer was the "bounce" effect noted when the direction was reversed during hysteresis measurements. As it turns out, these spurious signals were not a significant problem in the analysis of Wilhelmy balance data because data collected near turning points were discarded. Wetting forces in these regions are in an unstable transition from advancing to receding modes or *vice versa*.[7]

Operational Procedures. The *XYZ* robot was calibrated to precisely align with each of the 36 positions in the *XY* liquid-sample array (53 × 61 cm, see Figure 1B). The *Z* height span (51 cm) was adjusted to accommodate the plate-and-torsion-wire suspension, and 30-mL liquid samples were used in the experiments. Test liquid samples were held in 50-mL disposable polystyrene microbeakers (Fisher). This calibration ensured that the plate would neither bottom out at the maximum advancing depth nor break the fluid meniscus at the minimum receding depth when a hysteresis curve was recorded. A 10-s wait period was programmed after movement to each sample position to allow any motion of the plate-and-torsion-wire suspension to dampen.

Programming of the *XYZ* translation stage and therefore the protocols for making wetting measurements were very flexible with respect to the number of plate immersions, data acquisition rate, *Z*-motion velocity, etc. However, only three procedures were employed herein: four immersion cycles with and without plate rinsing between each sample and a one-cycle dip-and-hold method for measuring adsorption kinetics. In the four-immersion protocol, four advancing/receding cycles were recorded for the solid surface of interest in a single or multiplicity of liquid samples (see Figure 2 for example). When plate rinsing was required, an appropriate solvent was placed in the *XY* array (see Figure 1B) between each liquid sample. The robot was programmed to carry out a four-immersion protocol in the solvent without recording data. A 10-s hold period at the maximum immersion depth in the solvent was used in each of the four immersion cycles to further improve plate rinsing. Rinse volumes were 35 mL so that the plate was immersed slightly deeper during rinse steps than for each liquid sample (30 mL). When aqueous samples were studied, the rinses were either saline or deionized–distilled water, as appropriate to the sample series. When the liquid samples were organic fluids, trichlorofluoroethane was used as a rinse. It was found that this solvent quickly evaporated from the slide during travel from one sample location to another. Except where otherwise specifically noted, $\gamma_{(lv)}$ values reported herein are averages of the final two receding measurements of the four-immersion protocol.